

## Plasma-solution synthesis of a solid phase from solutions of iron and cobalt nitrates of various concentrations

*K.V. Smirnova\**, *D.A. Shutov*, *A.N. Ivanov*, *V.V. Rybkin*

*Ivanovo State University of Chemistry and Technology, Ivanovo, Russia*

*\*smirnovakv1@gmail.com*

**Abstract.** The solution of the fundamental problem of the physicochemical interaction of plasma with solutions of transition metal salts has practical applications in the field of creating new materials and purifying water from heavy metal ions. Plasma-solution synthesis has established itself as a simple and effective method for obtaining ultrafine materials with new properties. The formation of precipitation under the action of atmospheric pressure glow discharge on an iron and cobalt nitrates solution, which was the anode, was studied. It turned out that the rate of formation increases with an increase in the discharge current from 30 to 70 mA. In the course of work, the concentrations of nitrates were varied. The concentrations were chosen in such a way that the final product was stoichiometric  $\text{Fe}_2\text{O}_3 \cdot \text{CoO}$ . The result of the study of kinetic regularities indicates that the sedimentation of the solid phase from nitrate solutions occurs in two stages. The first is the precipitation of particles containing iron anions; the second capture is the precipitation of cobalt-containing particles.

**Keywords:** discharge, spinel, precipitate formation, kinetics

### 1. Introduction

Obtaining ultrafine spinels based on ferrites with a given ratio of components is an important research problem. Iron oxides of the spinel type are well known as hard magnetic materials with high cubic magnetocrystalline anisotropy, high coercive force, and moderate saturation magnetization [1]. Ferrites are an important class of composite oxide materials. Among various mixed materials, cobalt ferrite  $\text{CoFe}_2\text{O}_4$  is of particular interest due to its remarkable physical properties such as high magnetocrystalline anisotropy constant, high coercive force, moderate saturation magnetization, as well as good mechanical hardness and chemical stability, high catalytic activity, low cost and renewability. The characteristics of the composition and structure of ultrafine cobalt ferrites are described in the articles [2, 3]. Due to the unique properties, cobalt ferrites are applicable for high-density magnetic recording [4], power transformers and high-frequency microwave devices [5], as well as for catalysis of organic synthesis reactions [6], in medicine and the pharmaceutical industry [7].

Plasma synthesis from solutions is one of the simple and effective methods for obtaining nanomaterials. The wide distribution of plasma-solution systems is limited by the poor knowledge of the kinetics of processes in the "solution-discharge" system [8]. The attractiveness of such systems lies in the fact that when they act on water, a wide range of chemically active particles appear in it, which have both oxidizing and reducing properties [9]. The action of the discharge also leads to changes in the pH of solutions. Depending on the conditions, both acidic and alkaline environments can be obtained [10].

It can also be noted that the number of works devoted to the study of the kinetics and mechanisms of the formation of ultrafine materials under the action of gas discharges on solutions is extremely limited. The currently known works devoted to the synthesis of materials in plasma-solution systems are of a pronounced empirical nature [11].

The description of the processes occurring in a solution is often hypothetical in nature, not confirmed by experimental data. This paper presents the kinetic regularities of the formation of a solid phase in solutions of iron and cobalt nitrates under the action of a glow discharge of atmospheric pressure in air.

## 2. Experimental setup

### 2.1. Experimental setup for synthesis

In this work, we used aqueous solutions of iron and cobalt nitrates (analytical grade) with a different concentration for each component (Table 1). The plasma-chemical cell was an H-shaped quartz system separated by a cellophane membrane (Fig.1). Titanium electrodes were located above the surface of the solution at a distance of 5 mm. A high voltage sufficient for breakdown was applied to the titanium electrodes in such a way that the solution in one part of the cell becomes the liquid cathode, and in the other, the liquid anode. The volume of the solution in liquid anode and liquid cathode was equal to 100 ml. The discharge current was varying within 30–70 mA.

After 10 minutes of plasma treatment, the colloidal suspension was centrifuged, the resulting solid precipitate was dried in air at a temperature of 60 °C for 24 hours. The resulting powders were subjected to high-temperature treatment (900 °C for 1 hour), after which the elemental composition was obtained using the scanning electron microscope (SEM, Tesla Vega 3SBH, Czech Republic) with an EDX analysis system (Aztec EDS, Oxford Instruments Ltd., England).

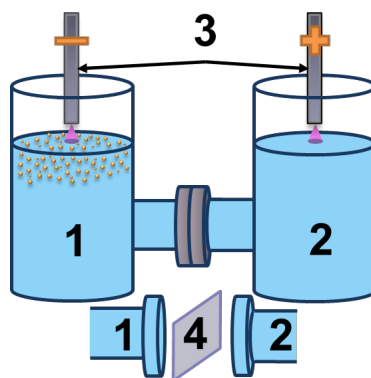


Fig.1. Scheme of the plasma-solution cell: 1 – Liquid anode (A); 2 – Liquid cathode (C); 3 – Titanium electrodes; 4 – cellophane membrane.

Table 1. Initial concentrations of solutions

| Sample number | Initial concentration of nitrate in %                |  | Concentration of initial nitrates in mmol/l          |  |
|---------------|--|--|--|--|
|               | Fe(NO <sub>3</sub> ) <sub>2</sub> ·9H <sub>2</sub> O | Co(NO <sub>3</sub> ) <sub>2</sub> ·6H <sub>2</sub> O | Fe(NO <sub>3</sub> ) <sub>2</sub> ·9H <sub>2</sub> O | Co(NO <sub>3</sub> ) <sub>2</sub> ·6H <sub>2</sub> O |
| FC-1          | 100  | 0  | 5  | 0  |
| FC-2          | 66   | 34   | 3.33   | 1.67   |
| FC-3          | 34   | 66   | 1.67   | 3.33   |
| FC-4          | 9  | 91   | 5  | 50   |
| FC-5          | 6  | 94   | 3  | 50   |
| FC-6          | 4.8  | 95.2   | 2.5  | 50   |
| FC-7          | 0  | 100  | 0  | 5  |

### 2.2. Experimental setup for turbidimetric measurements

In this work, a helium-neon laser with a wavelength of 632.8 nm was used for measurements. The laser was directed in such a way that intense radiation passed through the solution at a distance of 1 mm from its surface. The optical length was 45 mm. The AvaSpec-2048FT-2 spectrometer (Avantes, the Netherlands) was positioned relative to the radiation source and the plasma-solution cell as shown in Fig.2. The sample was irradiated with a beam of light with intensity  $I_0$ , and then the intensity of the transmitted radiation  $I_t$  was measured. As the number of suspension particles increases, the  $I_t/I_0$  ratio decreases. A detailed description and explanation of the technique of turbidimetric measurements for the processes of formation of a solid phase in a solution under the action of a gas discharge were given earlier [12, 13].

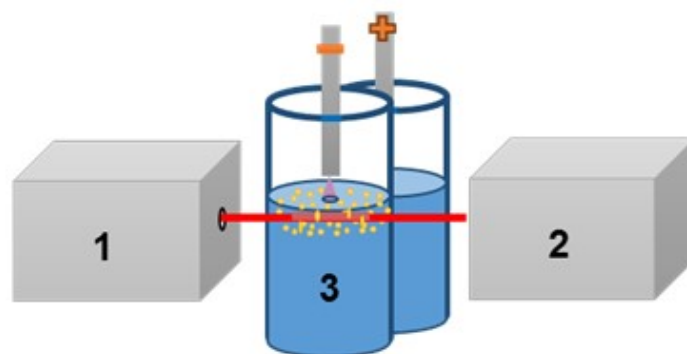


Fig.2. Scheme of turbidimetric measurements. 1 – radiation source, 2 – spectrometer, 3 – liquid anode.

### 3. Results and Discussion

During the first ten seconds, no visible changes were observed. Turbidimetric curves (Fig.3) illustrate the induction period of the process. After the induction period, the formation of colloidal particles began near the surface of the solution in the liquid anode (cell A) with further precipitation to the bottom of the cell. In a liquid cathode (cell C), no formation of colloidal particles was observed for cobalt nitrate solutions, but gas bubbles formed near the surface of the solution during treatment. In cases where iron nitrate was present in the solutions, the formation of a colloidal suspension was observed in both cells. However, studies show that the particles obtained in the cell C are not stable due to oxidative processes. Therefore, further description and discussion will focus on particles obtained in a liquid anode.

An increase in the discharge current leads to a decrease in the induction period (Fig.3). At a low value of the power put into the discharge, the induction period for the formation of Fe-containing powders is approximately twice as long as that for those containing Co, but as the discharge current increases, the induction period becomes comparable.

The Beer-Lambert law for intensity applies to turbidimetry:

$$I_T = I_0 e^{-a_T C}, \quad (1)$$

where  $I_T$  is the intensity of the transmitted light,  $I_0$  is the intensity of the light source,  $a_T$  is the proportionality factor, including the turbidity constant and the light path length,  $C$  is the concentration of particles on which the light is scattered.

In our case, the concentration is a function of the time the solution is treated by the discharge,  $C = C(t)$ . Let us assume that the kinetics of particle formation obeys a zero-order reaction:

$$C = kC_0 t, \quad (2)$$

where  $k$  is the effective rate constant for the formation of solid particles,  $C_0$  is the initial concentration of nitrate. Substituting equation (2) into expression (1) we get:

$$I_T = I_0 e^{-a_T k C_0 t} = I_0 e^{-K_T t}, \quad (3)$$

Indeed, the intensity kinetics of the transmitted light is well described by the first order equation (3) with an effective constant  $K_T$  of approximately  $10^{-2} \text{ s}^{-1}$  (pair correlation coefficient 0.98). Therefore, an increase in the discharge current leads to an increase in the constant. It should be noted that  $K_T$  characterizes not only the rate of formation of the solid phase, but also the processes of sedimentation.

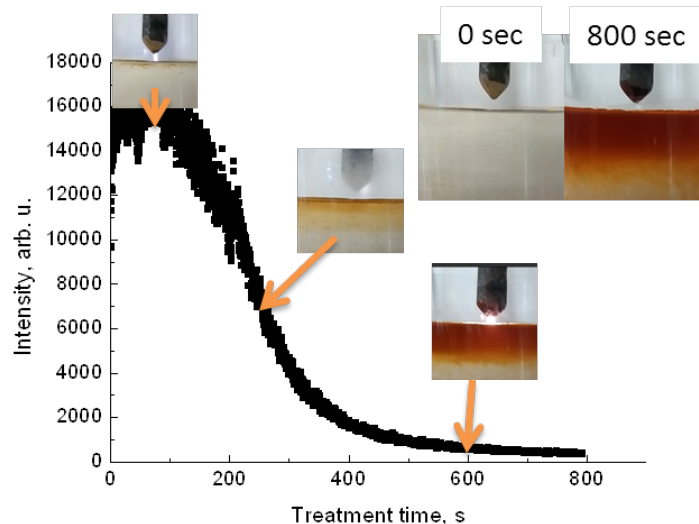


Fig.3. The dependence of the normalized transmission of the solution on the processing time. Discharge current is 50 mA. Initial concentration is FC-2.

The obtained dependences of the change in the rate constants of the formation of the solid phase on time were shown in Fig.4. As can be seen from the graph, the rate of formation of the solid phase in the solution under the action of the discharge increases with increasing current. In this case, a strong difference was observed only for the formation of particles in one-component solutions; for iron nitrate, the constants were higher than for cobalt nitrate. One of the reasons for the differences in the behavior of the solid phase formation constants in solutions of iron and cobalt nitrates on the discharge current was associated with a strong difference in the solubility product of hydroxides ( $K_{\text{Fe}(\text{OH})_3} = 3.8 \cdot 10^{-38}$ ;  $K_{\text{Co}(\text{OH})_2} = 1.6 \cdot 10^{-18}$ ) and, as a result, the initial pH value for the formation of insoluble compounds in the solution under the action of the discharge. Initial acidity value for precipitation for iron hydroxide  $\text{Fe}(\text{OH})_3$   $\text{pH} = 2.3$ , and  $\text{pH} = 7.6$  for cobalt hydroxide  $\text{Co}(\text{OH})_2$ . This was the main reason for choosing the initial concentrations of salt solutions.

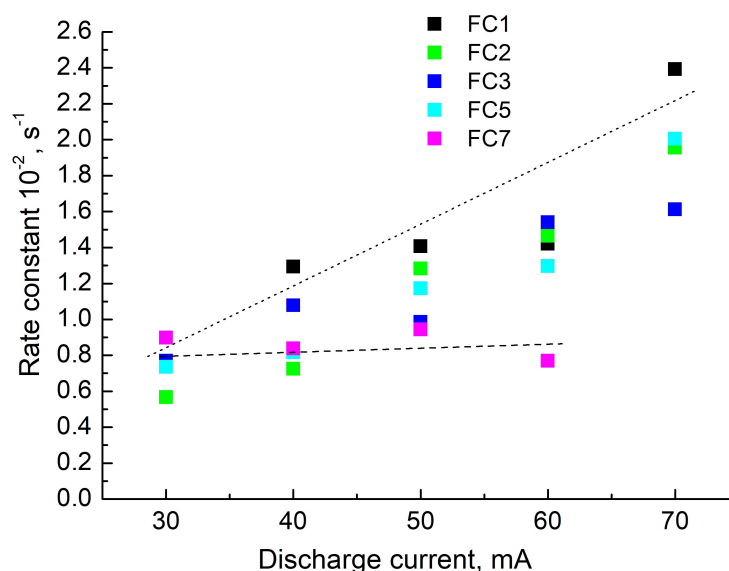


Fig.4. The dependence of the effective rate constant for the different initial concentration on the discharge current. The dots indicate the boundary conditions for the iron nitrate concentration of 100%. The dashes indicate the boundary conditions for a cobalt nitrate concentration of 100%.

Table 2 shows the results of energy dispersive analysis of the obtained powders after high-temperature treatment. As can be seen, a change in the concentration of the initial components leads to a change in the stoichiometric ratio of iron and cobalt in  $\text{CoFe}_2\text{O}_4$ .

**Table 2.** Comparison of initial concentrations of nitrates and formed oxides according to EDX data

| Sample number | Initial concentration of nitrate in %                |  | The content of the resulting oxides in% |              |
|---------------|--|--|---|--------------|
|               | $\text{Fe}(\text{NO}_3)_2 \cdot 9\text{H}_2\text{O}$ | $\text{Co}(\text{NO}_3)_2 \cdot 6\text{H}_2\text{O}$ | $\text{Fe}_2\text{O}_3$                 | $\text{CoO}$ |
| FC-1          | 100  | 0  | 100                                     | 0            |
| FC-2          | 66   | 34   | 99                                      | 1            |
| FC-3          | 34   | 66   | 76                                      | 24           |
| FC-4          | 9  | 91   | 60                                      | 40           |
| FC-5          | 6  | 94   | 50                                      | 50           |
| FC-6          | 4.8  | 95.2   | 26                                      | 74           |
| FC-7          | 0  | 100  | 0                                       | 100          |

#### 4. Conclusion

As a result of the work, the possibility of synthesizing cobalt ferrites from solutions of iron and cobalt nitrates under the action of a glow discharge at atmospheric pressure in air is shown. Using turbidimetry as an example, the kinetics of the formation of a solid phase in a solution under the action of plasma was studied. The settling rate of iron-containing particles is three times higher than that of cobalt-containing particles for solutions containing only one type of nitrate. Based on the data obtained, it can be concluded that the main contribution to the mechanisms of formation and precipitation is made by  $\text{Fe}^{3+}$  ions in solution. After high-temperature treatment of the resulting composites, we are dealing with pure oxides with a given stoichiometric ratio of iron and cobalt.

#### Acknowledgements

This work was supported by Russian Science Foundation № 22-22-00372 (rscf.ru/project/22-22-00372/, DS, VR, KS) and with the partial financial support of the Ministry of High Education and Science of the Russian Federation, project No. FZZW-2020-0009 (AI).

K. Smirnova thanks for the financial support the grant of the Russian Federation President (MK-2607.2022.1.2).

The study was carried out using the resources of the Center for Shared Use of Scientific Equipment of the ISUCT (with the support of the Ministry of Science and Higher Education of Russia, No. 075-15-2021-671).

#### 5. References

- [1] Amiri M., Salavati-Niasari M., Akbari A., *Adv. Colloid Interface Sci.* **265**, 29, 2019; doi:10.1016/j.cis.2019.01.003
- [2] Tatarchuk T., Bououdina M., Vijaya J.J., Kennedy L.J., *Springer, International Conference on Nanotechnology and Nanomaterials*, **195**, 305, 2016; doi: 10.1007/978-3-319-56422-7\_22
- [3] Qin H., et al., *Adv. Colloid Interface Sci.* **294**, 102486, 2021; doi: 10.1016/j.cis.2021.102486
- [4] Wang Z., Liu X., Lv M., Chai P., Liu Y., Meng J., *J. Phys. Chem. B*, **112**, 11292, 2008; doi: 10.1021/jp804178w
- [5] Hasegawa D., Yang H., Ogawa T., Takahashi M., *J. Magn. Magn. Mater.*, **321**, 746, 2009; doi: 10.1016/j.jmmm.2008.11.041
- [6] Casbeer E., Sharma V.K., Li X.-Z., *Sep. Purif. Technol.*, **87**, 1, 2012; doi: 10.1016/j.seppur.2011.11.034
- [7] Kim J.-E., Shin J.-Y., Cho M.-H., *Arch. Toxicol.*, **86**, 685, 2012; doi: 10.1007/s00204-011-0773-3
- [8] Saito G., Akiyama T., *J. Nanomater.*, **2015**, 123696, 2015; doi: 10.1155/2015/123696

- [9] Kruszelnicki J., Lietz A.M., Kushner M.J., *J. Phys. D: Appl. Phys.*, **52**, 355207, 2019; doi: 10.1088/1361-6463/ab25dc
- [10] Bruggeman P.J., Bogaerts A., Pouvesle J.M., Robert E., Szili E.J., *J. Appl. Phys.*, **130**:20, 200401, 2021; doi: 10.1063/5.0044261
- [11] Chen Q., Kaneko T., Hatakeyama R., *Phys. Express.* **5**, 6201, 2012; doi: 10.1088/0963-0252/20/3/034014
- [12] Shutov D.A., Smirnova K.V., Gromov M.V., Ivanov A.N., Rybkin V.V., *Plasma. Chem. Plasma Process.*, **38**, 107, 2018; doi: 10.1007/s11090-017-9856-0
- [13] Shutov D., Ivanov A., Rakovskaya A., Smirnova K., Manukyan A., Rybkin V., *J. Phys. D: Appl. Phys.*, **53**, 445202, 2020; doi: 10.1088/1361-6463/aba4d7.